



## The lithium oxide solubility in molten fluoride system CeF<sub>3</sub>–FLiNaK

IRINA ZAKIRYANOVA\*, IRAIDA KORZUN, ELENA NIKOLAEVA  
and ANDREY BOVET

Institute of High-Temperature Electrochemistry, 20 Akademicheskaya Street,  
Yekaterinburg, Russia

(Received 4 March, revised 17 March, accepted 27 March 2024)

**Abstract:** Molten systems based on alkali metal halides with lithium oxide additives are promising as a working medium on pyrochemical reprocessing of nuclear waste. A mixture of alkali metal fluorides of eutectic composition (FLiNaK) is a suggested solvent due to the high solubility of actinide oxides, low viscosity, high boiling points, low vapor pressure and resistance to radiation damage. Thermal analysis, XRD, Raman spectroscopy and thermodynamic simulations were used to obtain evidences on the phase equilibria and liquidus points of the system (0.85 FLiNaK–0.15 CeF<sub>3</sub>)–Li<sub>2</sub>O, containing up to 8.8 mol. % lithium oxide. The solubility of lithium oxide in the fluoride melt FLiNaK–CeF<sub>3</sub> and the thermodynamic parameters of dissolution were obtained. The eutectic point (the Li<sub>2</sub>O content is 3.1 mol. %,  $T_m = 489$  °C) and two peritectic points (lithium oxide content are 3.2 and 4.2 mol. %, and liquidus points are 497 and 549 °C, respectively) were found. Thermodynamic simulation results show an exothermic effect due to interaction between lithium oxide and fluoride melt. The interaction product oxyfluoride CeOF was detected by XRD analysis and Raman spectroscopy.

**Keywords:** lithium oxide; solubility; FLiNaK; cerium oxyfluoride; cerium fluoride; molten fluoride; phase diagram.

### INTRODUCTION

Pyrochemical reprocessing of spent nuclear fuel is one of the most promising options for environmentally safe handling of nuclear waste. It involves the electrolytic reduction process that converts the uranium oxide into metal in a molten salt electrolyte.<sup>1–6</sup> Oxide–halide melts based on alkali metal halides with lithium oxide additives are tested as a working medium. During the electrolysis of these melts, the released at the indifferent cathode lithium reduces actinide oxides to

\* Corresponding author. E-mail: optica96@ihte.ru  
<https://doi.org/10.2298/JSC240304038Z>

the corresponding metals.<sup>3,4,7</sup> For the process to proceed successfully, the concentration of lithium oxide must be at least 3 mol. %.<sup>7</sup>

The solubility of lithium oxide in LiCl and LiCl–KCl melts has been well studied.<sup>7–9</sup> It reaches 11.5 mol. % (923 K) for the LiCl solvent,<sup>5</sup> and decreases as potassium chloride is introduced into the solvent. In a melt of eutectic composition (58.5 LiCl–41.5 KCl) at 823 K, the solubility of lithium oxide is 1.32 mol. %.<sup>8</sup> The result presented in the literature<sup>7</sup> is interesting: it turns out that the addition of SrCl<sub>2</sub> (7 wt. %) enhance the Li<sub>2</sub>O solubility with respect to that in pure LiCl (from 8.8 to 9.1 wt. %).

There is little information on the solubility of lithium oxide in fluoride melts. It is reported in<sup>10</sup> that the solubility of lithium oxide in a melt of composition (0.8 LiF–0.2 CaF<sub>2</sub>) at a temperature of 1058 K is 10.6 wt. %, and increases on temperature increasing, reaching 14.8 wt. % at 1133 K.

Another promising solvent is a mixture of alkali metal fluorides of the eutectic composition LiF–NaF–KF (46.5–11.5–42 mol. %)–FLiNaK. Despite the fact that molten alkali metal fluorides are among the most aggressive to structural materials, it is the melts that have huge advantages due to high thermal conductivity, low viscosity, high boiling points, low vapor pressure, the highest heat capacity and stability to radiation damage. Unfortunately, the solubility of lithium oxide in the FLiNaK melt is low and is estimated to not exceed 1 %.<sup>11</sup>

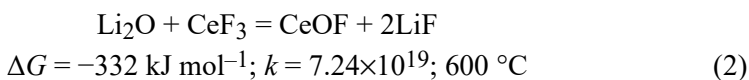
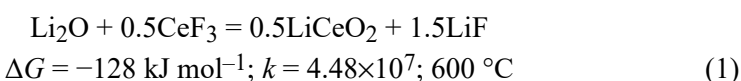
We may anticipate that the introduction of rare earth fluorides into a molten mixture of alkali metal fluorides will lead to an increase in the solubility of lithium oxide due to chemical interaction. The basis for this assumption are the results<sup>12</sup> indicating the solubility of rare-earth oxides in fluoride melts is extremely low, but abruptly increase when rare-earth fluoride is introduced into the melt. This result is associated with the interaction of the fluoride melt with rare-earth oxide during dissolution and the formation of oxide–fluoride complexes LnO<sub>x</sub>F<sub>y</sub>.<sup>13</sup>

In this work, as an example, we adopted the FLiNaK fluoride system with the addition of 15 mol. % cerium fluoride and studied the solubility of lithium oxide in this molten system.

First of all, when modeling the physicochemical behavior of plutonium compounds, cerium containing salts can be used as environmentally safe simulators.<sup>14,15</sup>

Next, the FLiNaK and FLiNaK–CeF<sub>3</sub> molten mixtures with small addition of Li<sub>2</sub>O were simulated within the *ab initio* theory to obtain the local structure patterns.<sup>16,17</sup> The introduction of cerium ions (in CeF<sub>3</sub>) into the oxide–fluoride melt, FLiNaK–Li<sub>2</sub>O, leads to significant changes in the parameters of the local structure: in the FLiNaK–CeF<sub>3</sub>–Li<sub>2</sub>O melt, cerium ions displace lithium from the immediate environment of oxygen. The longest-lived configuration includes oxygen, surrounded by cerium and lithium cations. The average lifetime of an O–Ce

ion pair exceeds 10 ps, while the average lifetime of an O–Li ion pair decreases from 5 (in FLiNaK–Li<sub>2</sub>O melt) to 1.1 ps. This change in the local structure and dynamics of ions of the oxide–fluoride molten system FLiNaK–CeF<sub>3</sub>–Li<sub>2</sub>O compared to the FLiNaK–Li<sub>2</sub>O melt allows, in particular, to make a prediction about the higher solubility of lithium oxide in melts containing cerium fluoride, compared to its solubility in FLiNaK. And finally, using the HSC Chemistry 9 software package,<sup>18</sup> we calculated the thermodynamic parameters of possible reactions of interaction of cerium fluoride with lithium oxide:



The calculation results showed negative values of the change of the Gibbs energy and large values of the thermodynamic reaction constant of the proposed reactions. It can be expected that the interaction of lithium oxide with CeF<sub>3</sub> dissolved in the fluoride melt will increase the solubility of lithium oxide.

The purpose of this study was to obtain information on the phase equilibria and liquidus points of the system (0.85 FLiNaK–0.15 CeF<sub>3</sub>)–Li<sub>2</sub>O, containing up to 8.8 mol. % lithium oxide; to determine the solubility of lithium oxide in the fluoride melt FLiNaK–CeF<sub>3</sub>, and to estimate the thermodynamic parameters of dissolution.

## EXPERIMENTAL

### *Experimental techniques*

Certification of the starting fluoride systems, determination of phase transformations points and accompanying thermal effects were carried out on a synchronous thermal analyzer STA 449C Jupiter coupled (NETZSCH, Germany). The instrument was calibrated using reference samples of RbNO<sub>3</sub>, KClO<sub>4</sub>, Ag<sub>2</sub>SO<sub>4</sub>, CsCl, K<sub>2</sub>CrO<sub>4</sub> and biphenyl C<sub>10</sub>H<sub>12</sub> (NETZSCH). The mass of the initial samples was 10–13 mg, the heating rate was 5 °C min<sup>-1</sup>. The temperature range for thermal analysis was 25–700 °C. To protect the device, measurements were carried out in a flow of protective gas (high purity Ar, 99.998 %). The gas flow rate was 20 ml min<sup>-1</sup>. The sample was placed in a Pt–Rh crucible with a pierced lid. According to the technical characteristics of the device, the error in determining the temperature was less than 1 °C, the error in measuring mass was 10<sup>-6</sup> g.

XRD analysis and Raman spectroscopy were used to certificate of CeF<sub>3</sub>, Li<sub>2</sub>O, and to identify reaction products. X-ray patterns were recorded using an automatic X-ray diffractometer Rigaku D/MAX-2200VL/PC (CuK<sub>α</sub> radiation, Rigaku MiniFlex 600 diffractometer, Tokyo, Japan), phases were identified using MDI Jade 6.5 software.

Raman spectra were recorded using the U1000 Raman microscope–spectrometer (Renishaw, UK) over a range 50–1000 cm<sup>-1</sup>, and Ava-Raman fiber-optic spectrometric complex (Avantes, Eerbeek, The Netherlands) over a range 150–5400 cm<sup>-1</sup>.

### *Reagents preparation and certification*

The eutectic mixture FLiNaK was prepared using extra pure LiF, NaF and potassium bifluoride KF·HF (Vekton Company, Saints Petersburg, Russia). It is known that when heated to 300–400 °C, the acid salt KF·HF decomposes with the formation of potassium fluoride and gaseous HF according to reaction:  $\text{KF}\cdot\text{HF} \rightarrow \text{KF} + \text{HF}\uparrow$ .

The formation of hydrogen fluoride is a positive factor affecting the purity of the obtained FLiNaK.<sup>19</sup> The required weighed portions of the initial reagents (LiF, NaF and KF·HF) were heated in a glassy carbon crucible at a rate of 2.5 °C min<sup>-1</sup> to a temperature of 750 °C and kept for 2 h, followed by cooling to room temperature. The melting point (460 °C) and enthalpy of melting of the obtained fluoride eutectic composition (414 J g<sup>-1</sup>, Fig. 1a) are consistent with the reference data.<sup>20</sup>

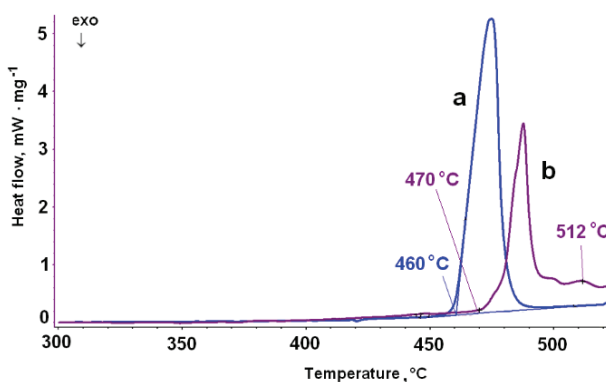


Fig. 1. The STA results: a) FLiNaK; b) 0.85 FLiNaK–0.15 CeF<sub>3</sub>.

The methods of Raman spectroscopy and XRD analysis were used to certify pure CeF<sub>3</sub> (99.9 %, CAS 7758-88-5, CHIMKRAFT Company, Russia). It is known that cerium fluoride under normal conditions has a crystal lattice of D<sub>3d</sub><sup>4</sup> symmetry, containing six formula units per unit cell. The selection rules determine 17 active modes (5A<sub>1g</sub> + 12E<sub>g</sub>) in the Raman spectrum.<sup>21</sup> Some of them, apparently, had weak intensity and were not recorded. In accordance with the results,<sup>21</sup> in the recorded spectrum of CeF<sub>3</sub> (Fig. 2a), the vibration bands at 396, 240, 295, 314 cm<sup>-1</sup> are associated with the A<sub>1g</sub> vibration modes, whereas those recorded at 77, 145, 203, 225, 306, 319, 386 cm<sup>-1</sup> are associated with E<sub>g</sub> modes. Vibration bands related to other phases, as well as bands of adsorbed water, were not found. XRD analysis of the used CeF<sub>3</sub> reagent also confirmed its single-phase nature (Fig. 2b). FLiNaK–CeF<sub>3</sub> mixtures, containing 15 mol. % of cerium fluoride, were prepared in a glove box in an inert atmosphere (Ar, moisture and oxygen content did not exceed 10 ppm). The mixtures of a given composition were exposed in a glassy carbon crucible for 5 h at the temperatures exceeding the liquidus point (512 °C)<sup>22</sup> of the studied compositions by 150–200 °C.<sup>22</sup> The STA analysis results of obtained mixture are shown in Fig. 1b. The solidus and liquidus points are consistent with the reference data.<sup>22</sup>

Lithium oxide was obtained by thermal decomposition of anhydrous lithium hydroxide.<sup>9</sup> In the Raman spectrum over the range 150–5400 cm<sup>-1</sup> of synthesized Li<sub>2</sub>O, the only one vibration band was noted at 524 cm<sup>-1</sup>, which is consistent with the data.<sup>23,24</sup> We note the active interaction of lithium oxide with water vapor and CO<sub>2</sub> in the air atmosphere. Fig. 3 shows the Raman spectra of a Li<sub>2</sub>O sample recorded sequentially when it was kept in an air atmo-

sphere. The formation of lithium hydroxide (vibration band at 3667 cm<sup>-1</sup>), crystalline hydrate, LiOH·H<sub>2</sub>O (3556 cm<sup>-1</sup>) and lithium carbonate (195, 1093, 1465 cm<sup>-1</sup>) were noticed. To prevent the formation of these impurities, the synthesized Li<sub>2</sub>O was stored in a glove box in an inert atmosphere.

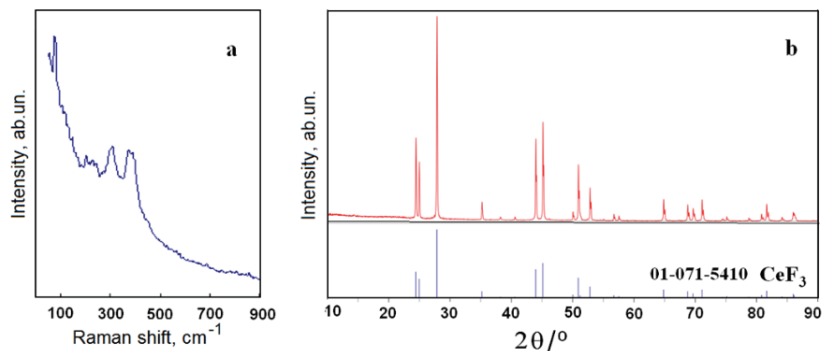


Fig. 2. Results of the cerium fluoride certification: a) Raman spectrum; b) XRD analysis.

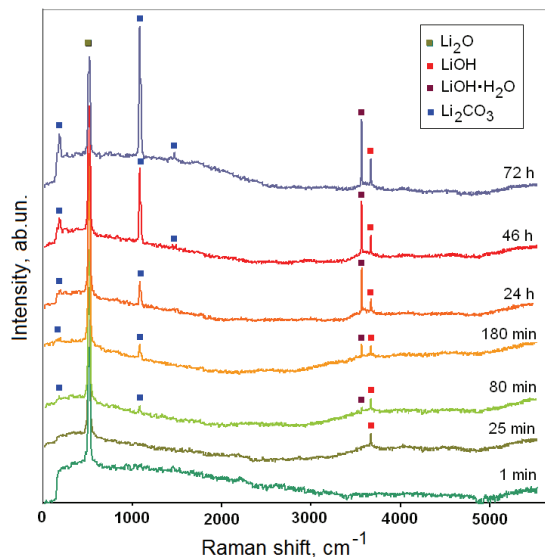


Fig. 3. Raman spectra of the Li<sub>2</sub>O on various exposure times in the air atmosphere. Products of interaction with water vapor and CO<sub>2</sub> are marked.

## RESULTS AND DISCUSSION

### *Phase equilibria and liquidus points of the (0.85 FLiNaK–0.15 CeF<sub>3</sub>)–Li<sub>2</sub>O system*

As an example, Fig. 4 shows several DSC curves obtained on studying the thermal behavior of the (0.85 FLiNaK–0.15 CeF<sub>3</sub>)–Li<sub>2</sub>O system. It can be seen that the introduction of lithium oxide into the fluoride system affects the number

of thermal effects and the phase transformations points. Taking into account the complete set of data obtained, the phase diagram of the system (0.85 FLiNaK–0.15 CeF<sub>3</sub>)–Li<sub>2</sub>O, containing up to 8.8 mol. % lithium oxide, was constructed (Fig. 5).

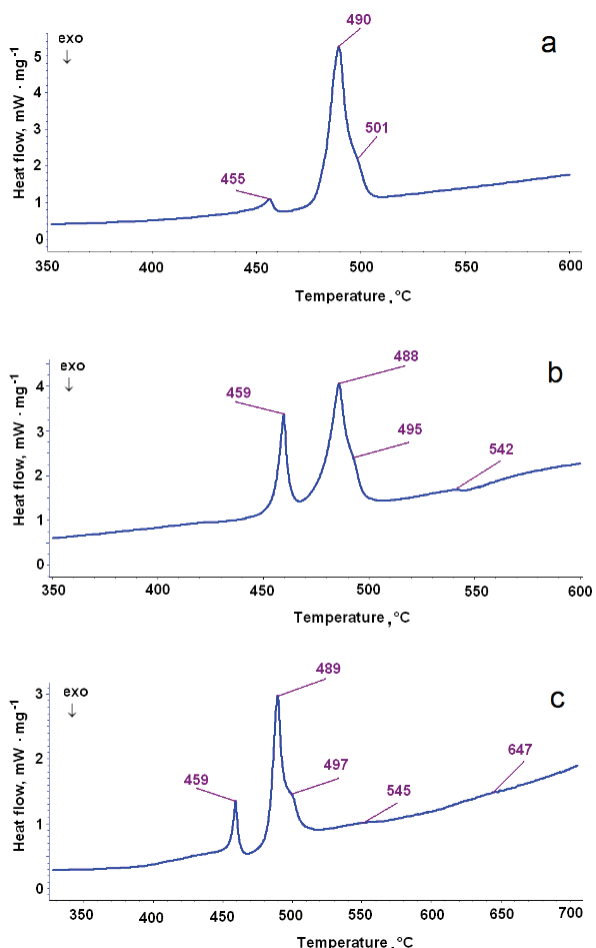


Fig. 4. DSC curves of the (0.85 FLiNaK–0.15 CeF<sub>3</sub>)–Li<sub>2</sub>O systems, containing 2.3 (a), 4.01 (b) and 8.8 mol. % (c) of lithium oxide.

In the system under study, the presence of a eutectic point was established (the Li<sub>2</sub>O content is 3.1 mol. %,  $T_m = 489$  °C), as well as two peritectic points (lithium oxide content 3.2 and 4.2 mol. %, and liquidus points 497 and 549 °C, respectively). The presence of the peritectic points indicates the formation in the system of thermally unstable incongruously melting compounds. The compositions of these compounds are outside the studied concentration range of the lith-

ium oxide. The solidus point of the system is 489 °C. An additional thermal effect was recorded at 456 °C, which can be associated with the polymorphic transformation of the oxyfluoride compound formed in the system. Using the XRD and Raman spectroscopy, a phase analysis of the frozen melts containing 3.5 mol. % Li<sub>2</sub>O, was carried out (Figs. 6 and 7).

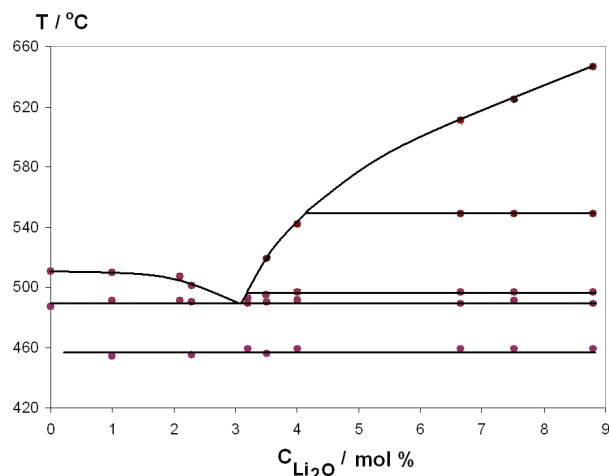


Fig. 5. Part of the phase diagram of the system (0.85 FLiNaK–0.15 CeF<sub>3</sub>)–Li<sub>2</sub>O.

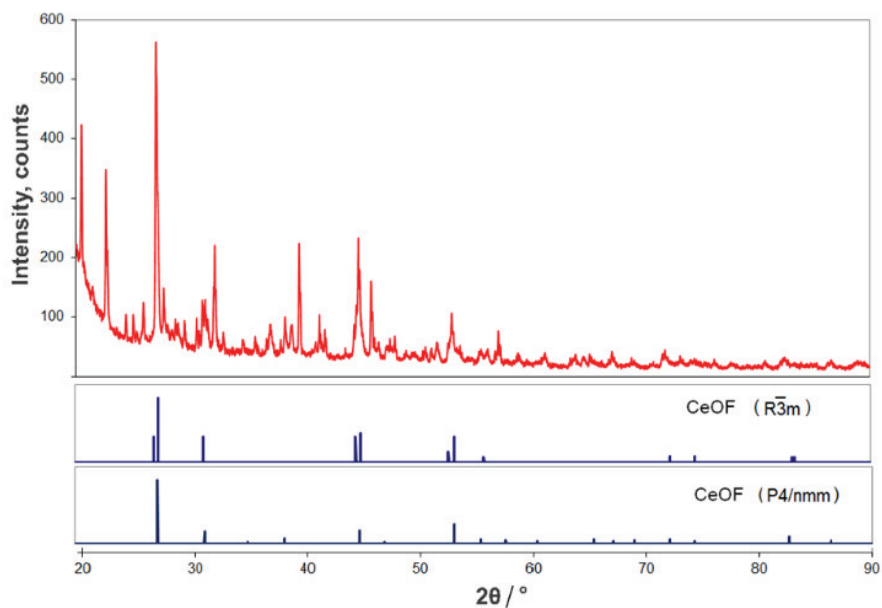


Fig. 6. XRD results of the frozen melt (0.85 FLiNaK–0.15 CeF<sub>3</sub>)–Li<sub>2</sub>O containing 3.5 mol. % of lithium oxide.

According to the XRD analysis, the presence of tetragonal (space symmetry group  $P4/nmm$ ) and rhombohedral (space symmetry group  $R\bar{3}m$ ) oxyfluorides CeOF (Fig. 6) were established. The Raman microspectroscopy confirms these results: for different microparticles of the sample, vibration spectra of CeOF associated with  $P4/nmm$  and  $R\bar{3}m$  space symmetry group<sup>25,26</sup> were recorded independently (Fig. 7).

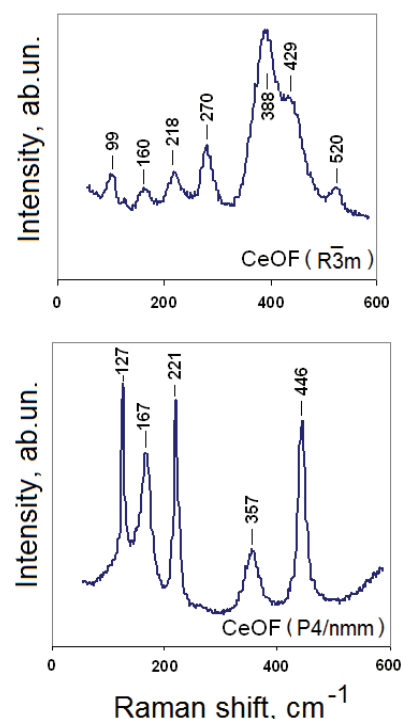


Fig. 7. Raman spectra of the different microparticles frozen melt (0.85 FLiNaK–0.15 CeF<sub>3</sub>)–Li<sub>2</sub>O containing 3.5 mol. % of lithium oxide.

The liquidus points of the oxide–fluoride system are presented in Table I. At first, the Li<sub>2</sub>O additions decrease the temperature of initial crystallisation and then increase it. The change of the dependence flow may be due to the new solid phase which was the first to crystallise during the melt cooling. For the present instance it should be the CeOF. The coordinates of the points on the ascending branches of the liquidus curve correspond to the lithium oxide solubility ( $S$ ) in the melt.

TABLE I. The liquidus points of the systems (0.85 FLiNaK–0.15 CeF<sub>3</sub>)–Li<sub>2</sub>O

Li <sub>2</sub> O content, mol. %	0	1	2.1	2.3	3.2	3.5	4.01	6.62	7.52	8.8
$T_{\text{liq}} / ^\circ\text{C}$	512	510	507	501	493	519	542	611	625	647

*Solubility of Li<sub>2</sub>O in 0.85 FLiNaK–0.15 CeF<sub>3</sub> molten system*

Using data on the liquidus points of the system (0.85 FLiNaK–0.15 CeF<sub>3</sub>)–Li<sub>2</sub>O, the lithium oxide solubility for different temperatures was calculated. The results are presented in Fig. 8. The Li<sub>2</sub>O solubility increases exponentially on the temperature increasing according to the equation:  $S = 0,078e^{0.0073T}$ , where  $T$  is the temperature in °C and  $S$  is Li<sub>2</sub>O solubility in mol. %.

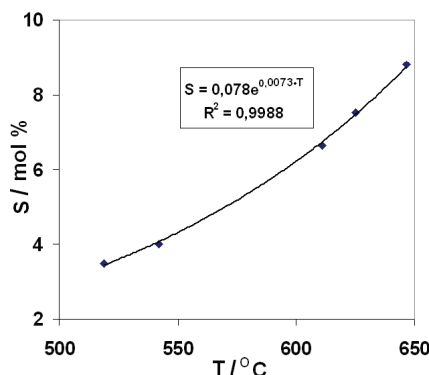


Fig. 8. The temperature dependence of Li<sub>2</sub>O solubility in fluoride molten system 0.85 FLiNaK–0.15 CeF<sub>3</sub>.

Fig. 9 shows the temperature dependence of Li<sub>2</sub>O solubility related to the ln  $S$ – $1/T$  coordinates over the temperatures 493–647 °C. It can be approximated by the linear equation:  $\ln S = A + B/T$ , where  $A$  and  $B$  are empirical coefficients:  $\ln S = 2.7598 - 4811.9/T \pm 0.04$ .

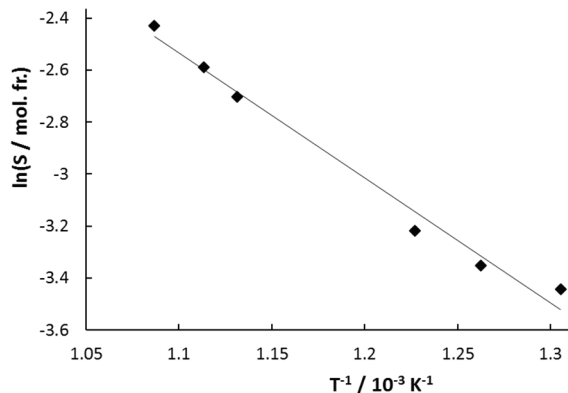


Fig. 9. The temperature dependence of Li<sub>2</sub>O solubility in 0.85 FLiNaK–0.15 CeF<sub>3</sub> molten system related to the ln  $S$ – $1/T$  coordinates.

The conditional value of the change in Gibbs energy of dissolution of 1 mol of the oxide,  $\Delta G^*_{\text{dis}}$ , is determined by the equation:

$$\Delta G^*_{\text{dis}} = -RT\ln K^* \quad (3)$$

where  $K^* = K/[f(\text{Li}_2\text{O})]$  is the conditional equilibrium constant of the dissolution process.  $K^*$  is equal to the  $\text{Li}_2\text{O}$  solubility ( $S$ , mol. fr.). At the same time for the studied  $\text{Li}_2\text{O}$  concentration range (up to 8.8 mol. %) the  $\text{Li}_2\text{O}$  activity coefficients  $f(\text{Li}_2\text{O})$  are assumed to be unchangeable.

Thus, we have obtained the following equation of the temperature dependence of the conditional change in Gibbs energy of dissolution:

$$\Delta G_{\text{dis}}^* = \Delta H^* - T\Delta S^* = -RT(A + B/T) \quad (4)$$

Accordingly, it is possible to calculate the conditional values of the change in enthalpy ( $\Delta H^* = -RB$ ) and entropy ( $\Delta S^* = RA$ ) when 1 mol of lithium oxide is dissolved in the melt (Table II).

TABLE II. The thermodynamic characteristics of  $\text{Li}_2\text{O}$  dissolution in fluoride molten system 0.85 FLiNaK–0.15 CeF<sub>3</sub>

$T$ °C (K)	$S$ mol. %	$\Delta G^*_{\text{sol}}$ $\text{J mol}^{-1}$	$\Delta H^*$ $\text{kJ mol}^{-1}$	$\Delta S^*$ $\text{J mol}^{-1} \text{K}^{-1}$	$\Delta G_m^{\circ 18}$ $\text{J mol}^{-1}$	$RT\ln(f(\text{Li}_2\text{O}))$ $\text{J mol}^{-1}$	$f(\text{Li}_2\text{O})$
500 (773)	3	22271			21644	-627	0.91
550 (823)	5	21124			20744	-380	0.95
600 (873)	6	19976	40.01	22.94	19774	-202	0.97
650 (923)	9	18829			18746	-83	0.99

Positive values of the enthalpy of dissolution indicate the endothermic effect of the process.

Based on these data, such thermodynamic parameters of dissolution as an excessive change in the Gibbs energy of mixing a liquid supercooled oxide with a molten solvent and the activity coefficients of  $\text{Li}_2\text{O}$  in the melt can also be determined.<sup>27,28</sup>

Let's consider the equilibrium of solid  $\text{Li}_2\text{O}(s)$  oxide and solution  $\text{Li}_2\text{O}(\text{sol})$  in a 0.85 FLiNaK–0.15 CeF<sub>3</sub> melt at a constant temperature:



Given the equality of the chemical potentials of solid and dissolved  $\text{Li}_2\text{O}$ , we have written:  $\mu^\circ(\text{Li}_2\text{O},s) = \mu(\text{Li}_2\text{O},\text{sol})$ . Here  $\mu(\text{Li}_2\text{O},\text{sol}) = \mu^\circ(\text{Li}_2\text{O},\text{liq}) + RT\ln a(\text{Li}_2\text{O},\text{sol})$ .

For the standard state for the solution, we take supercooled liquid lithium oxide at a given temperature, and:

$$\mu(\text{Li}_2\text{O},\text{sol}) = \mu^\circ(\text{Li}_2\text{O},\text{liq}) + RT\ln N(\text{Li}_2\text{O},\text{sol}) + RT\ln f(\text{Li}_2\text{O},\text{sol}) \quad (6)$$

Here  $N(\text{Li}_2\text{O},\text{sol})$  and  $f(\text{Li}_2\text{O},\text{sol})$  are concentration and activity coefficients of  $\text{Li}_2\text{O}$  in the melt.

Thus, we can write the change of Gibbs energy,  $\Delta G_m^\circ(T)$ , during  $\text{Li}_2\text{O}$  melting at temperature  $T$  by the equation:

$$\Delta G_m^\circ(T) = \mu^\circ(\text{Li}_2\text{O},\text{liq}) - \mu^\circ(\text{Li}_2\text{O},s) = -RT\ln N(\text{Li}_2\text{O},\text{sol}) - RT\ln f(\text{Li}_2\text{O},\text{sol}) \quad (7)$$

The change of the Gibbs energy on the dissolution process is expressed by the equation:

$$\Delta G^*_{\text{sol}}(T) = -RT\ln S = \Delta G^\circ_m(T) + RT\ln f(\text{Li}_2\text{O}, \text{sol}) \quad (8)$$

The  $RT\ln f(\text{Li}_2\text{O}, \text{sol})$  characterizes the excess changes of Gibbs energy of mixing of liquid overcooled oxide and a solvent melt.

The thermodynamic parameters of the Li<sub>2</sub>O dissolution in 0.85 FLiNaK–0.15 CeF<sub>3</sub> molten system calculated in this way using<sup>18</sup> and experimental solubility values are shown in Table II. Small negative values of  $RT\ln f(\text{Li}_2\text{O}, \text{sol})$  indicate an exothermic interaction between lithium oxide and solvent when mixed. With increasing temperature, the value of  $RT\ln f(\text{Li}_2\text{O}, \text{sol})$  takes on more positive values, which indicates a decrease in the exothermic effect of the interaction. Accordingly, the activity coefficients  $f(\text{Li}_2\text{O}, \text{sol})$  have values slightly lower than unity, which increase with temperature.

#### CONCLUSION

Pyrochemical reprocessing of nuclear fuel is the promising option for environmentally safe handling of nuclear waste. Molten systems based on alkali metal fluorides (FLiNaK) with lithium oxide additives are suggested as a working medium. The data on the solubility of lithium oxide in fluoride melts is in demand. DSC analysis, XRD, Raman spectroscopy and thermodynamic simulations were used to obtain evidences on the phase equilibria and liquidus points of the system 0.85 (FLiNaK–0.15 CeF<sub>3</sub>)–Li<sub>2</sub>O, containing up to 8.8 mol. % lithium oxide. The eutectic point (the Li<sub>2</sub>O content is 3.1 mol. %,  $T_m = 489$  °C) and two peritectic points (lithium oxide content are 3.2 and 4.2 mol. %, and liquidus points are 497 and 549 °C, respectively) were found. Using the DSC results on the liquidus points, the solubility of lithium oxide was determined. The temperature dependence of Li<sub>2</sub>O solubility ( $S$ , mol. %) is described by an equation:  $S = 0,078e^{0,0073T}$ . Thermodynamic simulation results show an exothermic effect due to interaction between lithium oxide and fluoride melt. The interaction product oxyfluoride CeOF was detected by XRD analysis and Raman spectroscopy.

*Acknowledgments.* The phase analysis was carried out by E. Vovkotrub and P. Mushnikov using the equipment of the Shared Access Center “Composition of Compounds” of the Institute of High Temperature Electrochemistry of the Ural Branch of the Russian Academy of Sciences. The preparation of lithium oxide was carried out by A. Mullabaev.

#### ИЗВОД

#### РАСТВОРЉИВОСТ ЛИТИЈУМ-ОКСИДА У РАСТОПУ ФЛУОРИДА CeF<sub>3</sub>–FLiNaK

IRINA ZAKIRYANOVA, IRAIDA KORZUN, ELENA NIKOLAEVA и ANDREY BOVET

*Institute of High-Temperature Electrochemistry, 20 Akademicheskaya Street, Yekaterinburg, Russia*

Растопи базирани на халогенидима алкалних метала уз додатке литијум оксида су потенцијално добра радна средина за пирохемијску додатну обраду нуклеарног отпада.

Смеша флуорида алкалних метала еутектичког састава (FLiNaK) је предложен растварац због високе растворљивости оксида актиноида, ниске вискозности, високих тачки кљу-чања, ниског напона паре и отпорности на оштећења од радијације. Термална анализа, XRD, раманска спектроскопија и термодинамичке симулације су коришћене да би се добили докази о равнотежи фаза и температури топљења система (0,85 FLiNaK–0,15 CeF<sub>3</sub>)–Li<sub>2</sub>O, који садржи 8,8 mol. % литијум-оксида. Одређена је растворљивост литијум-оксида у растопу флуорида FLiNaK–CeF<sub>3</sub> као и термодинамички параметри растварања. Нађене су еутектичка тачка (садржај Li<sub>2</sub>O је 3,1 mol. %,  $T_m = 489$  °C) и две перитактичке тачке (садржај литијум-оксида: 3,2 and 4,2 mol. % и тачке топљења: 497 и 549 °C, редом). Резултати термодинамичких симулација су показали егзотермни ефекат услед интеракција између литијум оксида и растопа флуорида. Производ интеракције је оксифлуорид CeOF који је детектован XRD анализом и раманском спектроскопијом.

(Примљено 4. марта, ревидирано 17. марта, прихваћено 27. марта 2024)

#### REFERENCES

1. H. Lee, G.-I. Park, K.-H. Kang, J.-M. Hur, J.-G. Kim, D.-H. Ahn, Y.-Z. Cho, E. H. Kim, *Nucl. Eng. Tech.* **43** (2011) 317 (<https://doi.org/10.5516/NET.2011.43.4.317>)
2. S. M. Jeong, B.H. Park, J.-M. Hur, C.-S. Seo, H. Lee, K.-C. Song, *Nucl. Eng. Tech.* **42** (2010) 183 (<https://doi.org/10.5516/NET.2010.42.2.183>)
3. E.-Y. Choi, C. Y. Won, D.-S. Kang, S.-W. Kim, *J. Radioanal. Nucl. Chem.* **304** (2015) 535 (<https://doi.org/10.1007/s10967-014-3842-2>)
4. Y. P. Zaikov, V. Y. Shishkin, A. M. Potapov, A. E. Dedyukhin, *J. of Physics: Conf. Series* **1475** (2020) 012027 (<https://doi.org/10.1088/1742-6596/1475/1/012027>)
5. M. Iizuka, T. Inoue, M. Ougier, J.-P. Glatz, *J. Nucl. Sci. Tech.* **44** (2007) 801 (<https://doi.org/10.1080/18811248.2007.9711869>)
6. B. H. Park, I. W. Lee, C. S. Seo, *Chem. Eng. Sci.* **63** (2008) 3485 (<https://doi.org/10.1016/j.ces.2008.04.021>)
7. D. Kim, S. Bae, J. Kim, T. Park, Y. Park, K. Song, *Asian J. Chem.* **25** (2013) 705 (<http://dx.doi.org/10.14233/ajchem.2013.18>)
8. Y. Kado, T. Goto, R. Hagiwara, *J. Chem. Eng. Data* **53** (2008) 2816 (<https://doi.org/10.1021/je800540c>)
9. A. Mullabaev, O. Tkacheva, V. Shishkin, V. Kovrov, Y. Zaikov, L. Sukhanov, Y. Mochalov, *J. Nucl. Mat.* **500** (2018) 235 (<https://doi.org/10.1016/j.jnucmat.2018.01.004>)
10. R. G. Reddy, S. G. Kumar, *Metal. Trans., B* **24** (1993) 1031 (<https://doi.org/10.1007/BF02660994>)
11. A. A. Maslennikova, P. N. Mushnikov, A. V. Dub, O. Y. Tkacheva, Y. P. Zaikov, Y.-L. Liu, W.-Q. Shi, *Materials* **16** (2023) 4197 (<https://doi.org/10.3390/ma16114197>)
12. X. Guo, J. Sietsma, Y. Yang, *A Critical Evaluation of Solubility of Rare Earth Oxides in Molten Fluorides*, in *Rare Earths Industry*, Eds.: I. B. De Lima, W. L. Filho, Elsevier, 2016, p. 223 (<https://doi.org/10.1016/B978-0-12-802328-0.00015-2>)
13. A. L. Rollet, E. Veron and C. Bessada, *J. Nucl. Mater.* **429** (2012) 40 (<https://doi.org/10.1016/j.jnucmat.2012.05.010>)
14. O. Beneš, R. J. M. Konings, *J. Nucl. Mater.* **435** (2013) 164 (<https://doi.org/10.1016/j.jnucmat.2012.12.005>)
15. R. Marsac, F. Réal, N. Banik, M. Pédrot, O. Pourret, V. Vallet, *Dalton Trans.* **46** (2017) 13553 (<https://doi.org/10.1039/C7DT02251D>)
16. D. Zakiryanov, *J. Mol. Liq.* **384** (2023) 122265 (<https://doi.org/10.1016/j.molliq.2023.122265>)

17. D. Zakiryanov, *Molecular Simul.* (2023) 845 (<https://doi.org/10.1080/08927022.2023.2193656>)
18. HSC Chemistry 9 Software, Outokumpu Research Oy, Pori, 2007
19. G. Zong, Z. Zhang, J. Sun, J. Xiao, *J. Fluor. Chem.* **197** (2017) 134 (<https://doi.org/10.1016/j.jfluchem.2017.03.006>)
20. J. Derek, Y. Toshinobu, J. Janz, *J. Chem. Eng. Data* **27** (1982) 366 (<https://doi.org/10.1021/je00029a041>)
21. R. P. Bauman, S. P. S. Porto, *Phys. Rev.* **161** (1967) 842 (<https://doi.org/10.1103/PhysRev.161.842>)
22. P. N. Mushnikov, O. Y. Tkacheva, A. S. Kholkina, Y. P. Zaikov, V. Y. Shishkin, A. V. Dub, *At. Energy* **131** (2022) 263 (<https://doi.org/10.1007/s10512-022-00876-2>)
23. F. S. Gittleson, K. Yao, D. G. Kwabi, S. Y. Sayed, W. Ryu, Y. Shao-Horn, A. D. Taylor, *ChemElectroChem* **2** (2015) 1446 (<https://doi.org/10.1002/celec.201500218>)
24. T. Osaka, I. Shindo, *Solid State Commun.* **51** (1984) 421 ([https://doi.org/10.1016/0038-1098\(84\)90126-1](https://doi.org/10.1016/0038-1098(84)90126-1))
25. E. M. Rodrigues, E. R. Souza, J. K. Monteiro, R. D. L. Gaspar, I. O. Mazali, F. A. Sigoli, *J. Mater. Chem.* **22** (2012) 24109 (<https://doi.org/10.1039/c2jm34901a>)
26. J. Hölsä, E. Säilynoja, H. Rahiala, J. Valkonen, *Polyhedron* **16** (1997) 3421 ([https://doi.org/10.1016/S0277-5387\(97\)00065-X](https://doi.org/10.1016/S0277-5387(97)00065-X))
27. E. V. Nikolaeva, I. D. Zakiryanova, A. L. Bovet, I. V. Korzun, *Z. Naturforsch.* **71** (2016) 731 (<https://doi.org/10.1515/zna-2016-0163>)
28. E. V. Nikolaeva, I. D. Zakiryanova, I. V. Korzun, A. L. Bovet, B. D. Antonov, *Z. Naturforsch.* **70** (2015) 325 (<https://doi.org/10.1515/zna-2014-0370>).